Available online at www.sciencedirect.com
ScienceDirect
Advances in Water Resources 31 (2008) 714–725
Advances in Water Resources
www.elsevier.com/locate/advwatres

Exposure concentration statistics in the subsurface transport

Roko Andricevic

Civil and Architectural Engineering Faculty, University of Split, Matice hrvatske 15, 21000 Split, Croatia

Received 4 June 2007; received in revised form 17 January 2008; accepted 20 January 2008
Available online 26 January 2008

Abstract

The concentration fluctuations resulting from hazardous releases in the subsurface are modeled through the concentration moments. The local solute exposure concentration, resulting from the heterogeneous velocity field and pore scale dispersion in the subsurface, is a random function characterized by its statistical moments. The approximate solution to the exact equation that describes the evolution of concentration standard moments in the aquifer transport is proposed in a recursive form. The expressions for concentration second, third and fourth central moments are derived and evaluated for various flow and transport conditions. The solutions are sought by starting from the exact upper bound solution with the zero pore scale dispersion and introducing the physically based approximation that allows the inclusion of the pore scale dispersion resulting in simple closed-form expressions for the concentration statistical moments. The concentration moments are also analyzed in the relative and absolute frame of reference indicating their combined importance in the practical cases of the subsurface contaminant plume migration. The influence of pore scale dispersion with different source sizes and orientations are analyzed and discussed with respect to common cases in the environmental risk assessment problems. The results are also compared with the concentration measurements of the conservative tracer collected in the field experiments at Cape Cod and Borden Site.

Keywords: Solute transport; Stochastic method; Concentration moments

1. Introduction

The concentration fields are of great interest in environmental flows and particularly in the subsurface flow. Many recent environmental regulatory initiatives stipulate that in order to improve the risk characterization, the ecological risk analysis needs to identify and conduct the probabilistic risk assessment. Potential toxicity of contaminated groundwater and associated health risk depend directly on exposure parameters and contaminant concentration values [27,33]. It is recognized that the high concentration values, with its duration and frequency of appearance, are responsible for a severe health risk and need to be predicted probabilistically. The fundamental concept in all methods used in probabilistic risk assessment consists of estimating the exposure concentration distribution and confront (using different methods) it to the distribution of effects obtained from the eco-toxicological studies. The tortuous and unpredictable pathways of groundwater flow resulting from geologic heterogeneity yield random concentration field. This randomness of the concentration field is common in all environmental flows; surface waters, atmosphere and groundwater. The fact that the concentration field is random has enormous consequence that the equations governing the evolution of the concentration field are rather challenging to solve.

The majority of previous studies focused on evaluating the concentration first two statistical moments using the first-order analysis, e.g., in terms of asymptotic perturbations within the Lagrangian framework [13,16,17,38,14,8,34,18] or the Eulerian truncation [20,25,21,22,31] or in combined Eulerian–Lagrangian concepts [28,37,39]. In each case, the concentration moments are derived following truncated perturbation or operator expansions differing only in the choice of a nominal value around which the perturbation is considered [26]. As an alternative, Andričević

E-mail address: rokoand@gradst.hr

0309-1708/$ - see front matter © 2008 Elsevier Ltd. All rights reserved.
doi:10.1016/j.advwatres.2008.01.007

[1] proposed the method of using spatially integrated concentration statistics to avoid velocity and spatial dependence and any form of truncation such that the closure is applied on the concentration gradient alone. All of these studies focused on deriving first two concentration moments under different flow conditions and using different way of accounting for the pore scale dispersion. The concentration mean and variance at the point in space and time describe the plume position and the fluctuation size within the plume structure. However, the exposure concentration probability density function (pdf) is an ultimate goal for assessing the practical risk coming from the toxic substances in the nature.

If only the mean and variance of concentration random process is available, the normal (or lognormal) distribution is a minimally prejudiced pdf that contains the largest amount of information [6,8]. The reality and some concentration measurements in other environmental media like air, and surface waters revealed the presence of a different concentration pdfs often exhibiting a bimodal shape, indicating two concentration peaks; one close to 0 where clean water was contaminated by diffusion from the plume core and the other one close to initial concentration representing those lenses and fingers containing the most of the initial mass. The concentration pdf can be constructed from knowledge of all of its moments such that higher moments weigh more heavily on extreme concentration events that are represented in the "tails" of the concentration pdf. Given the inherent difficulties in the subsurface transport problems it appears that the challenge is to define concentration statistics that have theoretically sound approach and have relevant information content which can be used in the practical cases.

In this paper we present simple, physically based approach to obtain solutions to the exact equations that describe the evolution of the moments of the probability density function of a conservative contaminant released in the subsurface flow. In particular, we derive the expression for evolution of first four moments of exposure concentration probability density function. The concentration moments are evaluated in the relative and absolute frame of reference and analyzed in terms of the influence coming form the pore scale dispersion, the source size and orientation. The derived concentration moments could be further used to estimate point or block pdf and confront it to some quality standards or eco-toxicological studies to assess the human health risk resulting from such concentration exposure. This paper modifies approach in [1] by replacing spatially integrated statistics and scaling function with new approximation introduced in Section 3, which allows a closed-form expression for the concentration higher moments.

The structure of this paper is as follows: in Section 2 we present the general problem description; in Section 3 the methodology for deriving the concentration moments is proposed; in Section 4 the illustrative examples are introduced and some results analyzed; in Section 4.1 the comparison with numerical studies is described; in Section 4.2 the effects from the source size and orientation are examined; in Section 5 the derived concentration statistics is evaluated and analyzed in the relative and absolute frame of reference; and finally the concluding remarks are given in Section 6.

2. Problem description

We consider incompressible and steady groundwater flow taking place through a heterogeneous aquifer rendering velocity and concentration field random and describable in statistical terms only. The mass conservation requires the resident concentration $c(\mathbf{x},t)$ to satisfy

$$\frac{\partial c(x,t)}{\partial t}+\nabla\cdot[\mathbf{v}(x,t)c(x,t)]=D\nabla^2c(x,t) \tag{1}$$

where $c(\mathbf{x},t)$ is defined as the mass per aquifer volume (of constant porosity) surrounding x at time t, $\mathbf{v}(\mathbf{x},t)$ is the groundwater velocity defined on the Darcy scale and $D\equiv D(x,t)$ is the pore scale dispersion (local dispersion) tensor commonly defined as $D(\mathbf{x},t)=D_{\mathrm{m}}I+\boldsymbol{\alpha}v(x,t)$ where D_{m} is an effective molecular diffusion and $\boldsymbol{\alpha}$ is a constant dispersivity tensor. A common approach in accounting for local dispersion is to replace $v(x,t)$ with the uniform ensemble mean, $\overline{v}(\mathbf{x},t)=E\{v(x,t)\}=U$ or to set D as a constant. Without loss of generality, we accept the later, e.g. [1,39].

The one-point probability density function of contaminant concentration is defined with $p(c;x,t)\,\mathrm{d}c=\mathrm{prob}\{c\leqslant c(x,t)\leqslant c+\mathrm{d}c\}$ and without sources and sinks the central moments are given by

$$\mu_n(\mathbf{x},t)=\int_0^\infty[c-m_1(\mathbf{x},t)]^np(c;\mathbf{x},t)\,\mathrm{d}c \tag{2}$$

where

$$m_n(\mathbf{x},t)=\int_0^\infty c^np(c;\mathbf{x},t)\,\mathrm{d}c \tag{3}$$

are standard moments. $m_1(\mathbf{x},t)$ denotes the mean concentration $\overline{c}(\mathbf{x},t)$ and for $n\geqslant 2$, μ_n can be expressed in terms of $m_n,\ldots,m_1$ such that for the concentration variance $\sigma_{\mathrm{c}}^2=\mu_2(\mathbf{x},t)=m_2-(m_1)^2$. In the absence of the pore scale dispersion, that is $D=0$, the concentration central moments are known functions of the mean concentration [12,9] and first few moments are

$$\mu_2(\mathbf{x},t)=\overline{c}(\mathbf{x},t)[C_0-\overline{c}(\mathbf{x},t)] \tag{4a}$$

$$\mu_3(\mathbf{x},t)=\overline{c}(\mathbf{x},t)[C_0-\overline{c}(\mathbf{x},t)][C_0-2\overline{c}(\mathbf{x},t)] \tag{4b}$$

$$\mu_4(\mathbf{x},t)=\overline{c}(\mathbf{x},t)[C_0-\overline{c}(\mathbf{x},t)][C_0^2-3C_0\overline{c}(\mathbf{x},t)+3\overline{c}^2(\mathbf{x},t)] \tag{4c}$$

In the subsurface flow there is a certain time span required for pore scale dispersion to become a dominant force in destroying the above exact moments for the $D=0$ case. As the source size gets smaller the required time for pore scale dispersion to become significant is getting larger. Therefore, the $D=0$ case can be regarded as a good

approximation for the near source condition and for as long as pore scale dispersion does not reduce significantly concentration moments. Since pore scale dispersion acts slowly compared to the advective velocity fluctuations, the $D = 0$ approximation provides a conservative envelope for the concentration moments.

3. Methodology for concentration moments expressions

By multiplying (1) with $c^n(x,t)$ and taking the ensemble average, the concentration mass balance in terms of standard moments can be written as

$$\frac{\partial}{\partial t} m_{n+1} + \nabla \cdot \overline{v c^{n+1}} = D\nabla^2 m_{n+1} - n(n+1) D \overline{c^{n-1} (\nabla c)^2} \qquad (5)$$

where n is the order of standard moments considered, overbar denotes an ensemble average and dependence on $(\mathbf{x}, t)$ is omitted for easier notation. The pore scale dispersive term $D\nabla^2 m_{n+1}$ is very much smaller than the advective term $\nabla \cdot \overline{v c^{n+1}}$ and will be neglected. Since the pore scale dispersive process acts very slowly compared to the heterogeneous advective velocity, we will estimate the advective term for the $D = 0$ case.

For the zero local dispersion case and for uniform initial concentration $c(0,0) = C_0$, the concentration pdf follows from:

$$p(c; \mathbf{x}, t) = [1 - f(\mathbf{x}, t)]\delta(c) + f(\mathbf{x}, t)\delta(c - C_0) \qquad (6)$$

where $f(\mathbf{x}, t)$ denotes the particle displacement pdf and $\delta(\cdot)$ is Dirac delta function. This pdf says that for $D = 0$ one has weighted two states of concentration; one being in fluid phase of zero concentration and another in fluid phase of initial concentration. The pore scale dispersion is the only process that is smoothing out these two states of concentration values.

The exact standard moments for $D = 0$ case are given with $m_{n+1}(\mathbf{x}, t) = C_0^n \overline{c}(\mathbf{x}, t)$. Following the reasoning by Sullivan [36], we use this expression for exact standard moments in (5) to arrive at the expression for the advective term for the zero local dispersion case:

$$\nabla \cdot \overline{v(\mathbf{x}, t) c^{n+1}(\mathbf{x}, t)} = -C_0^n \frac{\partial \overline{c}(\mathbf{x}, t)}{\partial t} \qquad (7)$$

This assumption is constant with the fact that groundwater flows are mostly laminar and pore scale dispersion acts very slowly in destroying the upper limit moments, leaving (7) particularly justifiable for the near-field subsurface transport. Using (7) in (5) the concentration mass balance in terms of standard moments becomes

$$\frac{\partial}{\partial t} m_{n+1} - C_0^n \frac{\partial \overline{c}}{\partial t} = -n(n+1) D \overline{c^{n-1} (\nabla c)^2} \qquad (8)$$

Reduction of the release conservative concentration $c(0,0) = C_0$ occurs only through the pore scale dispersion. In saturated heterogenous aquifers the advective velocity field pulls and stretches the solute plume by conveying the released mass through lenses and fingers of higher velocities. This process creates the concentration gradient along which the pore scale dispersion acts as diffusion process diluting high concentration and fattening the lenses and fingers [23]. As transport time progresses the two processes balance each other at some effective scale λ_c [1], which at large time correspond to actual scale of developed fingers and lenses (see Plate 1 in [5]). The dynamics of concentration fluctuations [21] and geological characteristics of the aquifer with connectivity structure will affect the size of λ_c which has finite possible range $0 < \lambda_c \ll I$, where I is the hydraulic conductivity correlation scale. The scale of concentration fluctuation dynamics has full analogy in atmospheric diffusion where balance between turbulent convective motions and molecular diffusion is achieved around the Batchelor conduction cut-off length which is 10^{-3}–10^{-5} m for most flows and also supported with several experimental results [9].

The geological characteristics of the aquifer and its connectivity structure will affect the size of λ_c. In practice, λ_c can be estimated through borehole measurements using in situ dilution tests, geophysical logging and by labeling the whole water column with tracers [30]. Alternatively, λ_c may be estimated numerically with $\lambda_c = \int_0^\infty S_c(k)\mathrm{d}k / \int_0^\infty k^2 S_c(k)\mathrm{d}k$, where $S_c(k)$ is the power spectrum of c obtained from the fine grid (e.g., $\leqslant 0.1I$) at given time and k is the wave number. Using this alternative approach, one may solve numerically only one realization of the mean concentration over the subdomain to get λ_c estimate which can then be used to evaluate the concentration higher moments at any domain size. The significant values of $(\nabla c)^2$ are expected to be present only over thin lenses and fingers characterized with the developed λ_c scale such that the gradient approximation is

$$\nabla c(\mathbf{x}, t) = \frac{c(\mathbf{x}, t) - c^*(t)}{\lambda_c(t)} \qquad (9)$$

where $c^*(t)$ is a background threshold concentration such that $c^*(t) \to 0$ as $t \to 0$ and $c^*(t) \to \overline{c}(x,t)$ as $t \to \infty$. The later case, as in [1], will be used to close (8) together with $\lambda_c(t)$ assumed to remain constant over the plume at large time t. This assumption of large time is related to the slow acting local dispersion and balances out the assumption used for the advective term (advective term evaluated for $D = 0$ case) in (7) which applies not only at early time, but also whenever the solute mass is advancing in the new region of the host fluid assuming the slow acting local dispersion mechanism. This is particularly true for the subsurface flow where solid and liquid phase are spatially mixed and inherently limit the mixing process compared to other one phase environmental media.

Using (9) in (8) results in a suitable form of the governing equation for the concentration standard moments with $n \geqslant 1$:

$$\frac{\partial}{\partial \tau} m_{n+1} + \frac{n(n+1)}{\gamma^2 Pe} [m_{n+1} - 2\overline{c} m_n + \overline{c}^2 m_{n-1}] = C_0^n \frac{\partial \overline{c}}{\partial \tau} \qquad (10)$$

where $\tau = \frac{tU}{I}$ is dimensionless time, $Pe = UI/D$ is the Peclet number, and $\gamma = \lambda_c / I$ is a scale factor between concentration

(gradient) scale and log-conductivity correlation scale. Eq. (10) is a first-order linear homogeneous ordinary differential equation which has solution in the form

$$m_{n+1}(\mathbf{x},\tau) = C_0^n\overline{c}(\mathbf{x},\tau) + \kappa a\exp(-\kappa a\tau)\int_0^\tau \overline{c}(\mathbf{x},\zeta) \times \exp(\kappa a\zeta)\cdot[2m_n(\mathbf{x},\zeta) - \overline{c}(\mathbf{x},\zeta)m_{n-1}(\mathbf{x},\zeta) - C_0^n]\,\mathrm{d}\zeta \tag{11}$$

where $\kappa = n(n+1)$ and $a = (\gamma^2 Pe)^{-1} = \frac{DI}{U\lambda_c^2}$ is dimensionless parameter that represents the ratio between the local dispersion and flow conditions described with concentration scale λ_c. For an infinite Peclet number (e.g., zero local dispersion case) a equals zero and (11) reduces to $m_{n+1}(\mathbf{x},t) = C_0^n\overline{c}(\mathbf{x},t)$; exact expression for concentration standard moments for $D = 0$. The magnitude of a in (11) determines the strength of local dispersion process. Expression in (11) is in recursive form and can be potentially used to evaluate any number of concentration standard moments needed.

The second, third and fourth concentration central moments follow from (11) as

$$\mu_2(\mathbf{x},\tau) = \overline{c}(\mathbf{x},\tau)[C_0 - \overline{c}(\mathbf{x},\tau)] + 2a\exp(-2a\tau) \times \int_0^\tau \overline{c}(\mathbf{x},\zeta)\exp(2a\zeta)[\overline{c}(\mathbf{x},\zeta) - C_0]\,\mathrm{d}\zeta \tag{12a}$$

$$\mu_3(\mathbf{x},\tau) = \overline{c}(\mathbf{x},\tau)[C_0 - \overline{c}(\mathbf{x},\tau)][C_0 - 2\overline{c}(\mathbf{x},\tau)] + 6a\exp(-6a\tau)\int_0^\tau \overline{c}(\mathbf{x},\zeta)\exp(6a\zeta) \times [2m_2(\mathbf{x},\zeta) - \overline{c}^2(\mathbf{x},\zeta) - C_0^2]\,\mathrm{d}\zeta - 6a\overline{c}(\mathbf{x},\tau)\exp(-2a\tau) \times \int_0^\tau \overline{c}(\mathbf{x},\zeta)\exp(2a\zeta)[\overline{c}(\mathbf{x},\zeta) - C_0]\,\mathrm{d}\zeta \tag{12b}$$

$$\mu_4(\mathbf{x},\tau) = \overline{c}(\mathbf{x},\tau)[C_0 - \overline{c}(\mathbf{x},\tau)][C_0^2 - 3C_0\overline{c}(\mathbf{x},\tau) + 3\overline{c}^2(\mathbf{x},\tau)] + 12a\exp(-12a\tau) \times \int_0^\tau \overline{c}(\mathbf{x},\zeta)\exp(12a\zeta) \times [2m_3(\mathbf{x},\zeta) - \overline{c}(\mathbf{x},\zeta)m_2(\mathbf{x},\zeta) - C_0^3]\,\mathrm{d}\zeta - 24a\overline{c}(\mathbf{x},\tau)\exp(-6a\tau) \times \int_0^\tau \overline{c}(\mathbf{x},\zeta)\exp(6a\zeta) \times [2m_2(\mathbf{x},\zeta) - \overline{c}^2(\mathbf{x},\zeta) - C_0^2]\,\mathrm{d}\zeta + 12a\overline{c}^2(\mathbf{x},\tau)\exp(-2a\tau) \times \int_0^\tau \overline{c}(\mathbf{x},\zeta)\exp(2a\zeta)[\overline{c}(\mathbf{x},\zeta) - C_0]\,\mathrm{d}\zeta \tag{12c}$$

In comparison with (4a)–(4c) it is clear that above derived moments are having the first term on the right hand side representing the exact solution for $D = 0$ and the remaining terms represent the dilution effect coming from $D \neq 0$. This solution is equally applicable to other environmental flows where concentration scalar is introduced or incidentally released.

4. Illustrative examples

Consider the case of a pulse injection over a finite volume Ω_0. To evaluate derived concentration moments, consider the Gaussian distribution of mean concentration in the form

$$\overline{c}(\mathbf{x}^r,\tau) = MC_0(\tau)\exp\left(-\frac{Y_1^2}{2Y_{11}} - \frac{Y_2^2}{2Y_{22}} - \frac{Y_3^2}{2Y_{33}}\right) \tag{13}$$

where $C_0(\tau) = [(2\pi)^{3/2}(Y_{11}Y_{22}Y_{33})^{1/2}]^{-1}$, Y_i is the particle displacement relative to the center of mass, and Y_{ii} denotes the relative displacement variance. From now on the spatial coordinate vector $\mathbf{x}^r$ denotes the coordinate system relative to the plume center such that solutions in (12a)–(12c) will be evaluated in the relative frame of reference. For example, for a planar source of size $A_0 = h_x \times h_y$, the relative displacement variance follows from the two-particle analysis [e.g., [4]].

$$Y_{ii} = \frac{Y'_{ii}}{I_Y^2} = 2\int_0^\tau (\tau - \tau')C_{u_i}(\tau',0,0)\,\mathrm{d}\tau' - \frac{2}{A_0^2}\int_{A_0}\int_{A_0}\int_0^\tau (\tau - \tau')C_{u_i}(\tau',\beta_y,\beta_z)\,\mathrm{d}\tau'\,\mathrm{d}\beta_y\,\mathrm{d}\beta_z \tag{14}$$

where C_{u_i} denotes the normalized velocity covariance, i.e., $C_{u_i} = \overline{u'_i u'_i}/U^2$, β_i is an initial separation between particles, and $\tau = tU/I$. The relative displacement variance was previously analyzed by Kitanidis [24], Dagan [10,11], Rajaram and Gelhar [33] and Zhang et al. [39].

Using (13) and setting $C_0 = MC_0(0)$ creates initial small inconsistency which is not great since a uniform source quickly develops into a Gaussian profile [35]. This can also be seen as placing a uniform source at some distance upstream. The initial source concentration $MC_0(0)$ will be used as normalizing constant in presented examples.

In Figs. 1a–1c the comparison is made between concentrations moments for the zero local dispersion case (4a)–(4c) and general solution (12a)–(12c) for μ_2, μ_3 and μ_4, respectively. The second, third and fourth concentration moments are evaluated along the plume centerline along the flow direction and for the two-dimensional source scaled by I, such that $h_x = 0.2$ and $h_y = 1.0$. Each profile for concentration moments is presented for four different travel times, $\tau = 1, 2, 5$, and 10. The solid thin line in all figures represents the upper limit solution given in (4a)–(4c). The concentration moments are normalized with the initial source concentration of unit mass and displayed as a function of dimensionless distance from the source. Two levels of the pore scale dispersion strength are considered ($a = 0.01$ and 0.1). The concentration variance for $a = 0.01$ case is still close to the upper limit defined with (4a) while third and fourth concentration moments are showing some more pronounced effect from the presence of the local dispersion. It is clear that the pore scale dispersion is diluting (reducing) the higher concentration moments the most. This characteristic is even more

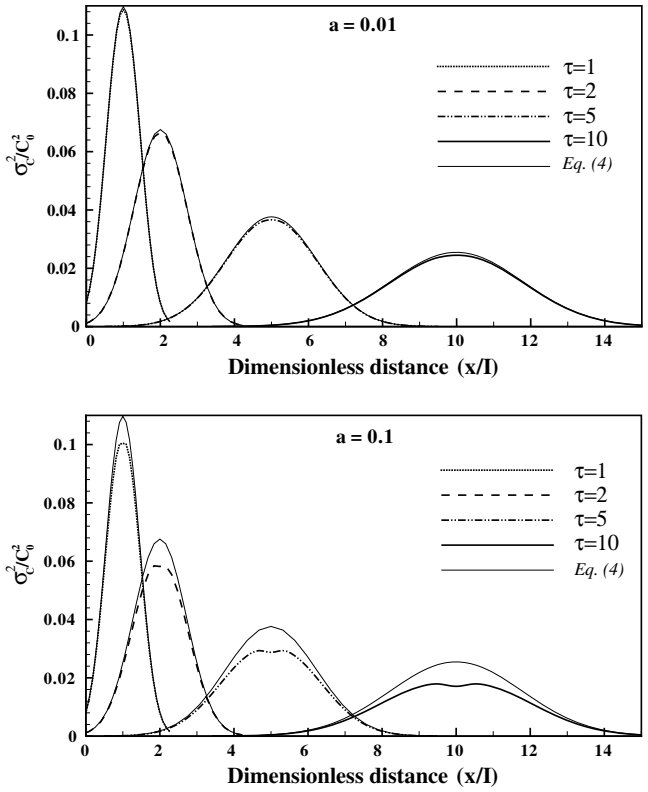

Fig. 1a. Normalized concentration variance for four travel times compared with the upper limit (4).

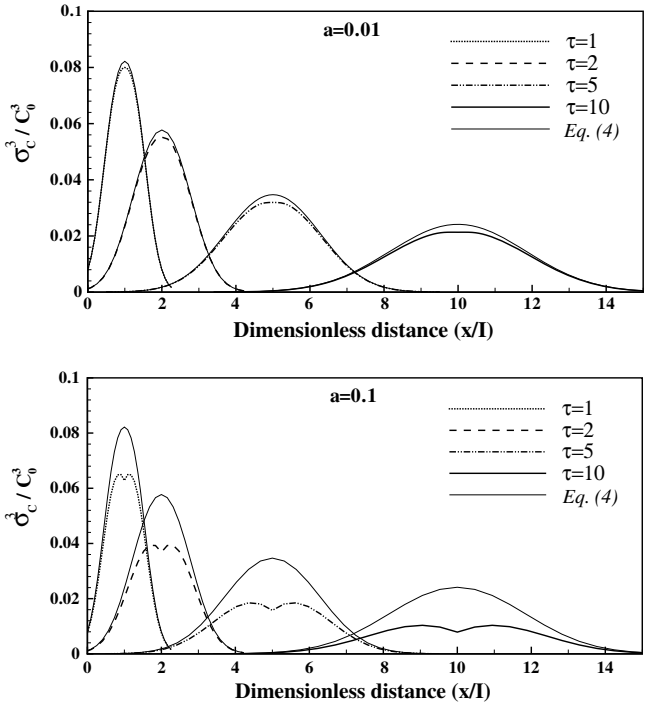

Fig. 1b. Normalized third concentration moment for four travel times compared to upper limit (4).

pronounced as we increase the local dispersion strength with $a = 0.1$. This result is expected based on physical grounds (larger local dispersion, larger the reduction in

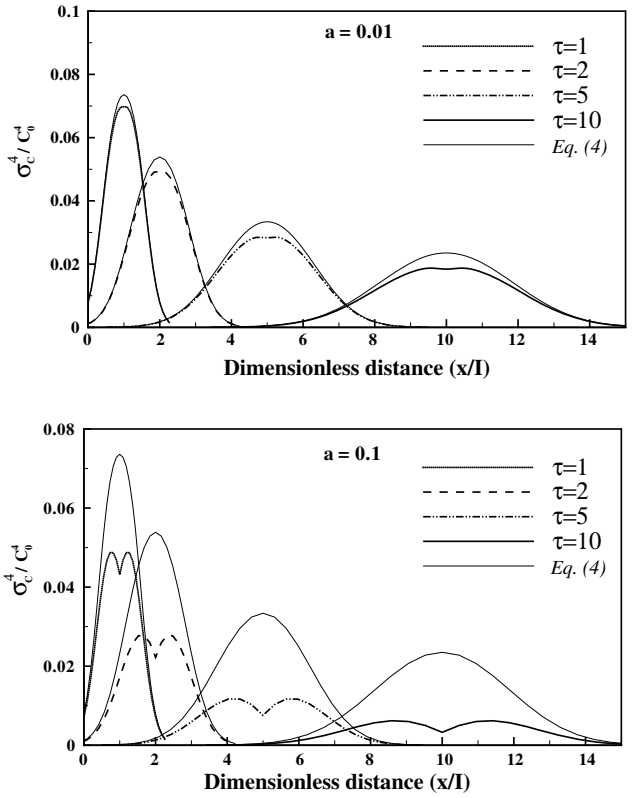

Fig. 1c. Normalized third concentration moment for four travel times compared to upper limit (4).

concentration moments) and it is also expressed in the derived solutions (12a)–(12c). The concentration moments spatial distribution for $a = 0$ are following unimodal shape whereas the $a \neq 0$ cases are often exhibiting the bimodal shape for the second, third and fourth concentration moments.

Figs. 2a–2c are displaying the second, third and fourth concentration moments in the transverse direction along the plume center. The effects from the local dispersion in diluting the higher concentration moments are also present. The form of the concentration moments are maintaining the unimodal shape even for larger strength coming from local dispersion. Besides the local dispersion, the sampling volume is also the mechanism that creates additional dilution of concentration moments [1] and should not be overlooked when comparing the theoretical results with field or laboratory measurements.

4.1. Comparison with the field-case studies

In the subsurface flow and transport studies it is very rare to find concentration statistics based on the field measurements. This is particularly true for concentration higher moments. Unfortunately, exactly those higher concentration moments are providing information about possible existence of thin lenses filled with the contaminant mass that can adversely affect the groundwater quality and human health. Those areas if intercepted by water

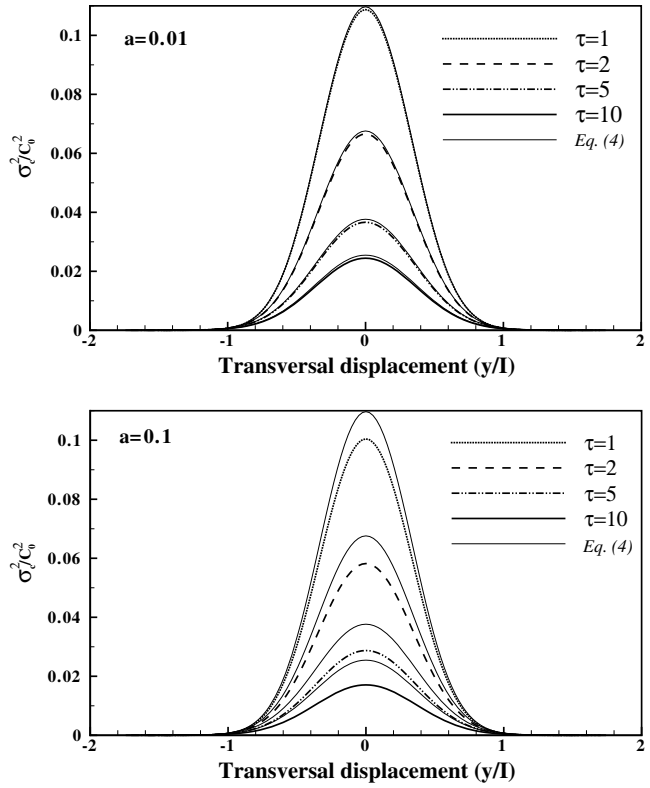

Fig. 2a. Transversal profile of normalized concentration variance for four travel times compared to upper limit (4).

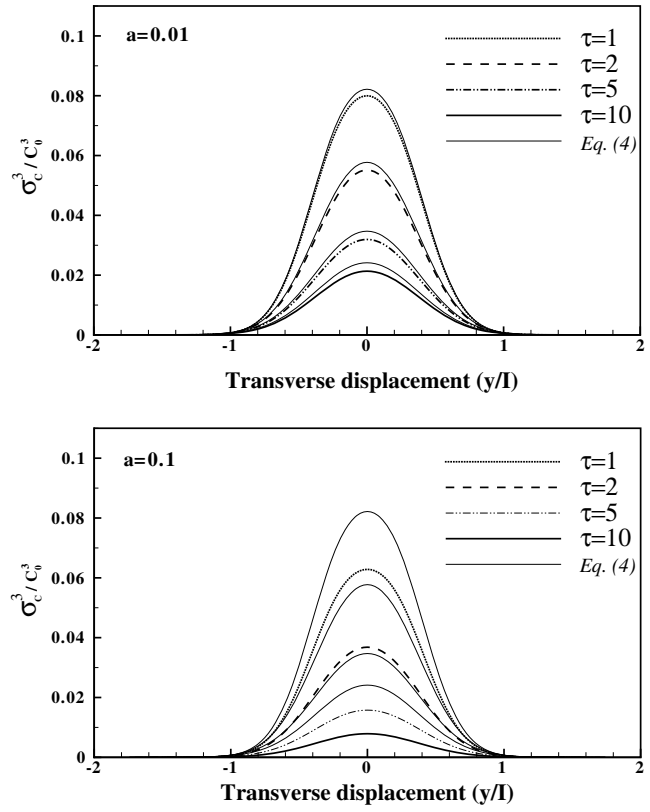

Fig. 2b. Transversal profile of normalized concentration third moment for four travel times compared to upper limit (4).

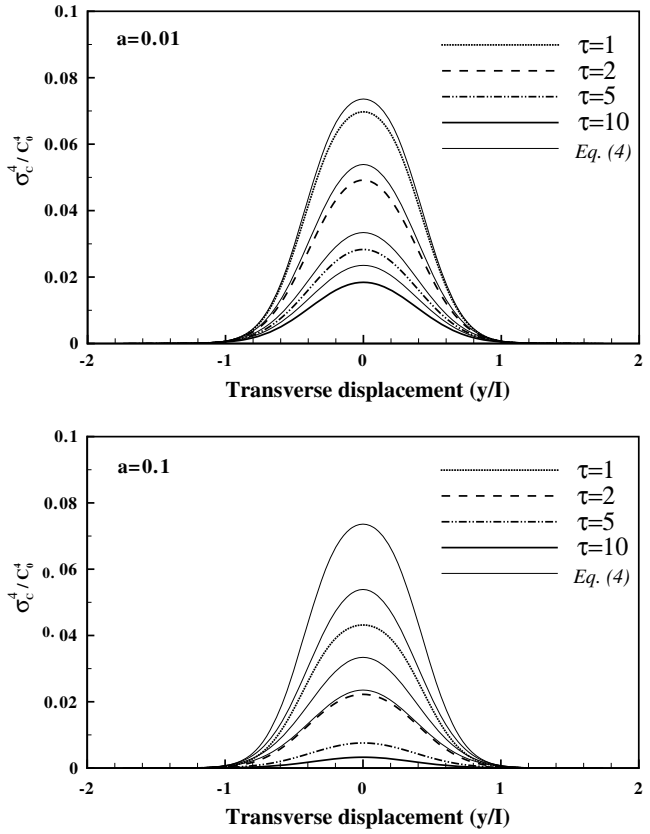

Fig. 2c. Transversal profile of normalized concentration fourth moment for four travel times compared to the upper limit (4).

supply wells or discharged in some recipient can create the severe risk by exposing some population to high mass during some prescribed time.

For the purpose of comparison, the presented formulation for the concentration variance (12a) is compared with the concentration measurements of the conservative tracer (bromide) collected in the field experiments at Cape Cod (CC) and Borden Site (BS). Fitts [19] statistically analyzed the concentration measurements from CC and BS introducing the variable $F = \ln[c(x,t)/c_m(x,t)]$ which was found to follow approximatively normal distribution $N[0,\sigma_F^2]$. Fitts [19] defines $c_m(x,t)$ as modeled concentration which is derived analytically from (1) assuming the advection by the mean velocity and plume spreading controlled by the constant macrodispersion coefficients $D_{ii} = A_{ii}U$. The modeled concentration $c_m(x,t)$ is given by the analytical solution [19, Eq. (4)]:

$$c_m(x,t) = C_0\omega(x_1)\omega(x_2)\omega(x_3)$$
$$\omega(x_i) = \frac{1}{2}\left[\operatorname{erf}\left(\frac{x_i - U_i t + h_i/2}{2\sqrt{D_{ii}t}}\right) - \operatorname{erf}\left(\frac{x_i - U_i t - h_i/2}{2\sqrt{D_{ii}t}}\right)\right] \quad (15)$$

The statistical analysis of F was done by comparing $c_m(x,t)$ with actual observed concentration limiting pairs to the low concentration threshold of 0.3 mg/l. Following the Fitts' [19] assumption of the lognormality of c the standard deviation of $\ln(c/c_m)$ is given with [16]

$$\sigma_F = [\ln(1 + \sigma_c^2/\overline{c}^2)]^{1/2} \quad (16)$$

By assuming that the field-case plumes at CC and BS are ergodic in terms of σ_F we can exchange the spatial average (reported by Fitts [19, Table 3]) with the ensemble average. The computation of the plume average of σ_F is achieved by the volume integration of (16) constrained with the cut-off value of 0.3 mg/l. The same approach in comparing the second concentration moment with Fitts [19] data was presented in [16].

In Fig. 3a the experimental results for Cape Cod test in terms of σ_F as a function of time is compared to three levels of transverse dispersivity. The results indicate that $\alpha_T = 5$ mm used in some previous studies seems to overestimate the mixing process in the average sense while $\alpha_T = 1.5$ mm (as suggested by Fitts [19]) shows good agreement with data. Lower transverse dispersivity of $\alpha_T = 0.5$ mm begins to underestimate the mixing process on average at the Cape Coda data.

In Fig. 3b a similar comparison is presented for the Borden Site experiment. Three values of transverse dispersivities are examined. Again, the previously used value of $\alpha_T = 5$ mm shows increased mixing compared to data, whereas $\alpha_T = 1$ mm shows good agreement with experimental data. This comparison shows that value of $\alpha_T = 2.2$ mm, as suggested by Fitts [19], only in the early stage of transport confirms with the data while for the later stage shows increased mixing in the average sense.

In this comparison only transverse macrodispersivity α_T was varied while all other variables were taken from the independently determined data of the two plumes. The dimensionless parameter appearing in (12a) that controls the strength of the local dispersion is attributed in this example to the vertical transverse dispersivity and was evaluated with $a = \alpha_T I_3/\lambda_c^2$.

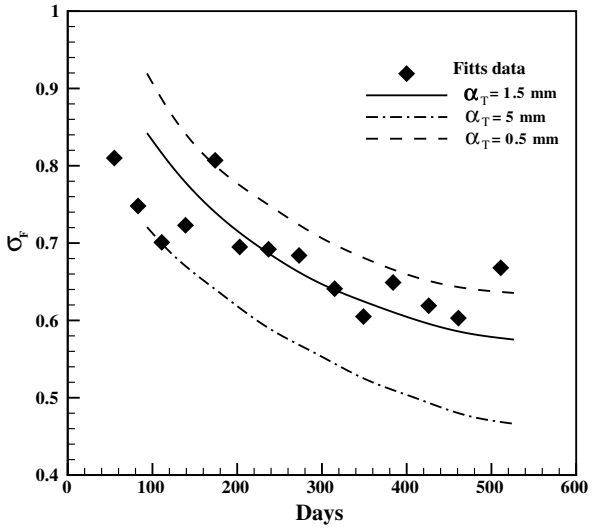

Fig. 3a. Comparison between the Cape Cod field experimental $\overline{\sigma}_F$ [19] (solid diamonds) and theoretical σ_F for different values of transverse local dispersivity using $\log_{10}$ in (16).

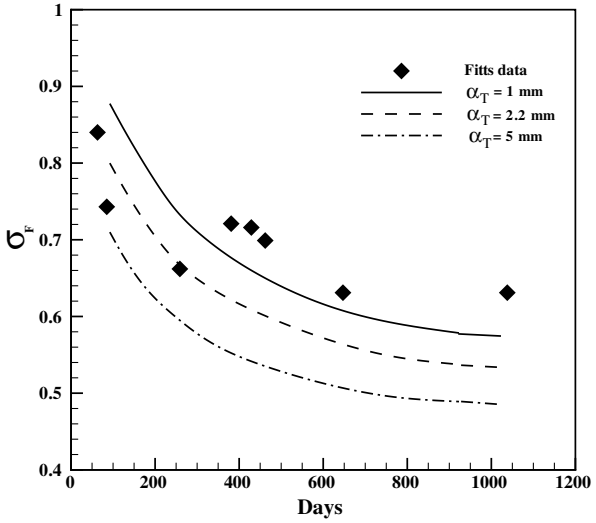

Fig. 3b. Comparison between the Borden Site field experimental $\overline{\sigma}_F$ [19] (solid diamonds) and theoretical σ_F for different values of transverse local dispersivity using $\log_{10}$ in (16).

This statistical analysis of the plume average value of σ_F is highly dependent of the concentration cut-off threshold since (16) increases rapidly in plume tails. Therefore, the oscillations found in the Fitts' [19] data may be due to the fixed limited sampling of the moving plume besides some possible nonergodicity. The agreement between the experiment and theory should be viewed in the context of comparing the plume average value of (16) under assumption of lognormal concentration pdf. To compare the theory with experiments for higher order concentration moments, derived in (12b) and (12c), is a future challenge which will also help to check the validity of the lognormal assumption.

In addition, the presented formulation for the concentration variance (12a) was compared with the numerical simulations of Burr et al. [7, Fig. 7]. They performed numerical examination of the actual field-scale transport by groundwater at the Borden Site. The proposed expression for concentration variance in (12a) showed very good qualitative agreement with the numerical results of Burr et al. [7] particularly in confirming the bimodal shape that was clearly detected in the numerical simulations and in (12a). The bimodal profile for concentration moments, appearing in solution (12a)–(12c), results as combined effect between the magnitude of local dispersion and time needed for advection process to stretch and distort the plume.

4.2. Effects from the source size and orientation

The source size and its orientation with respect to the mean flow direction also have significant effect on the evolution of concentration moments. The concentration moments are having different magnitude and different spatial support depending on the source size and orientation. Using (13) and (14), modified to account for injection over a finite volume [6], the normalized concentration variance

is presented in Fig. 4 as a function of four different source sizes defined with $A_0(x,y)$. The x coordinate is aligned in the mean flow direction. Since the concentration moments are derived in the relative frame of reference, the source size of $A_0(0.1,0.1)$ denotes almost the point source and majority of concentration variability in space is attributed to the meandering of the plume and only small portion of velocity heterogeneity on the scale of order 0.1 and less is creating the concentration variance presented with the dotted line in Fig. 4. It is interesting to note that the significant source width in the mean flow direction (on order of $\ln K$ correlation scale), regardless whether we have square source or line source in the direction of the mean flow, yields the concentration variance much higher than in any other cases examined.

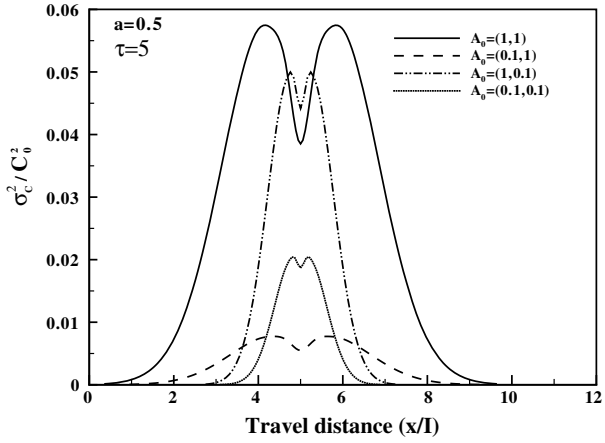

Fig. 4. Normalized concentration variance as a function of travel distance for four different source sizes and orientation.

Figs. 5a–5c display the second third and fourth concentration central moments field for the case of thin line source placed perpendicular to the mean flow direction $A_0(0.2,1)$ (bottom) and line source aligned with the mean flow $A_0(1,0.2)$ (top) for the local dispersion parameter $a = 0.1$. The line source aligned with the mean flow generates larger magnitude of the concentration moments with bimodal peak placed close to each other. On the other hand, the line source perpendicular to the mean flow also exhibits the bimodality with larger separation between peaks, which is becoming even more pronounced for the higher order concentration moments.

There will always be a large uncertainty about the source size and general flow conditions when accidental release happens in the subsurface and in any other environmental media. The scientific ability to predict the exposure concentration fluctuations is very limited even under perfect knowledge of source size and orientation and any methodology that is theoretically sound and consistent is valuable tool for risk assessment and management.

5. Concentration statistics in absolute frame of reference

The exposure concentration moments derived in ((12a)–(12c)) are provided in the relative frame of reference due to

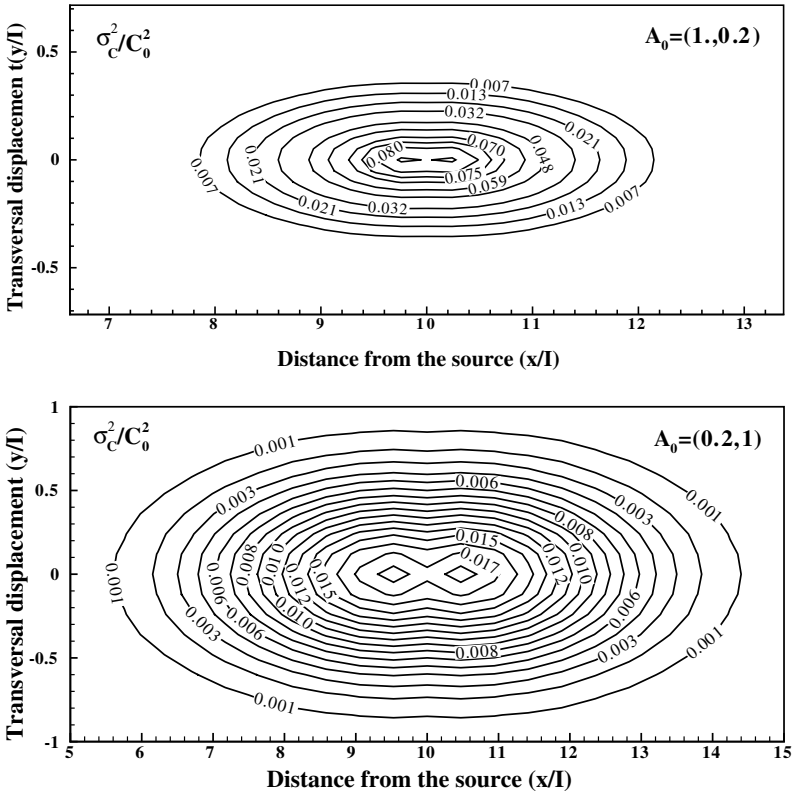

Fig. 5a. 2-D plot of normalized concentration variance for two different source orientation.

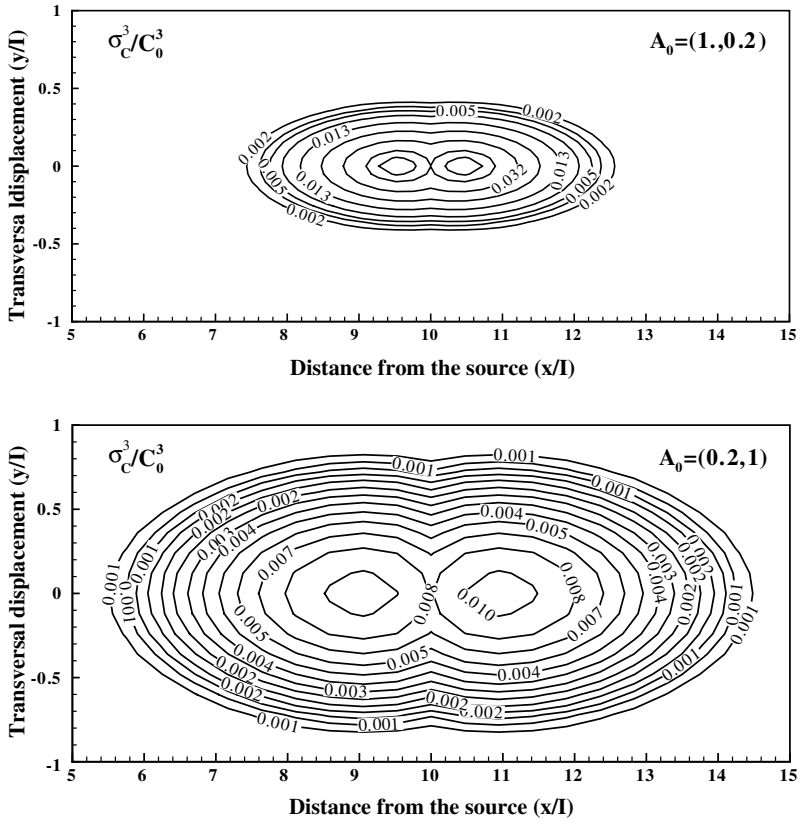

Fig. 5b. 2-D plot of normalized concentration third moment for two different source orientation.

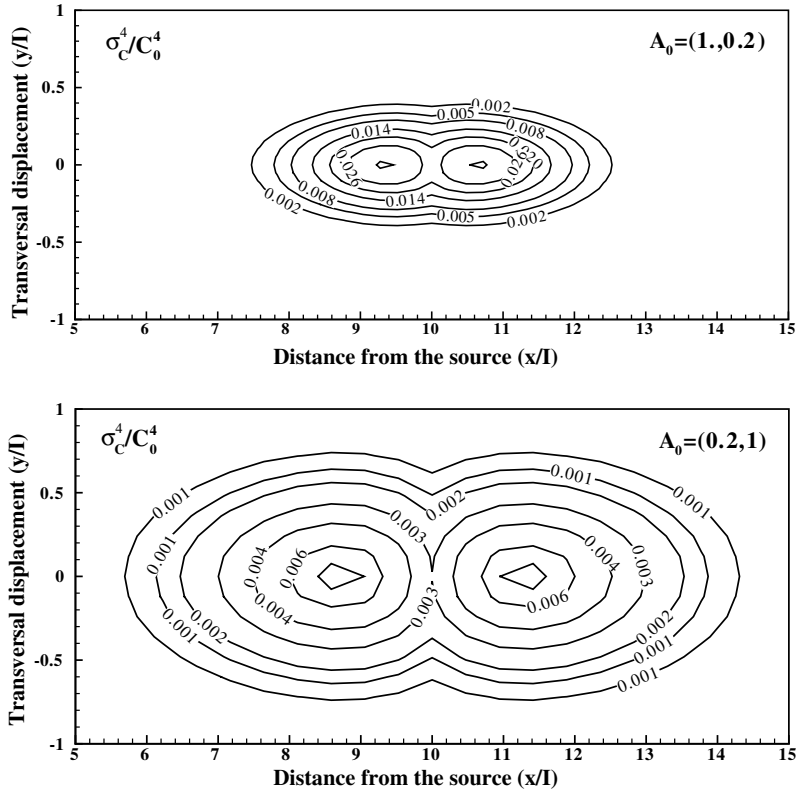

Fig. 5c. 2-D plot of normalized concentration fourth moment for two different source orientation.

the expression for the mean concentration field (13). The results presented up to now are in the relative frame of reference and indicate the plume advection and dispersion process generated with the velocity heterogeneity scale on the order of the instantaneous plume dimension and smaller. The large scale meandering of the plume (created with the heterogeneity scale on order of the plume size and larger) was removed from the absolute displacement variance (e.g., the second term on the right hand side of (14)). However, when modeling and predicting the exposure concentration statistics in the practice, either for the environmental risk assessment studies or monitoring network design, the model output or prediction is often sought in the absolute frame of reference. The extreme fluctuations that accumulate a certain amount of injected mass within lenses and fingers are responsible for a risk in groundwater pollution problems only if the plume is passing near the supply well. Thus, the main aim of this section is to introduce the way how to convert the relative framework results, so far explained, to the absolute frame of reference.

Consider the notation that at each time t the contaminant concentration field at position $\mathbf{x} = (x_1, x_2, x_3)$, denoted with $c(\mathbf{x}, t)$, has a position vector of the plume center denoted as $R(t) = [R_1 = X_1^C, R_2 = X_2^C, R_3 = X_3^C]$, where

$$\left(X_1^C, X_2^C, X_3^C\right) = M^{-1} \int\int\int_{\mathbb{R}^3} x_1, x_2, x_3 c(\mathbf{x}, t)\, \mathrm{d}x_1\, \mathrm{d}x_2\, \mathrm{d}x_3 \tag{17}$$

At each time t, it is now possible to redefine the absolute frame of reference (see Fig. 6) as $x = x^r + R$ such that the concentration field relative to the plume center $c(\mathbf{x}^r, t) = c(\mathbf{x} - R, t)$. Furthermore, $R, c^r,$ and c can be considered as stationary random variables, in the subsurface transport, each having its own pdf.

Hence, the absolute frame one-point concentration pdf $p(c; \mathbf{x}, t)$ can be related to the relative frame pdf $p^r(c; \mathbf{x}^r, t)$ through the spatial convolution relationship (e.g., [29])

$$p(c; x, t) = \int\int\int_{\mathbb{R}^3} p^r(c; x^r, t) p_R(x - x^r; t)\, \mathrm{d}x_1^r\, \mathrm{d}x_2^r\, \mathrm{d}x_3^r \tag{18}$$

where p_R denotes the pdf of the plume center position. From (18) the relationship between concentration moments in absolute frame of reference and relative moments can be obtained directly:

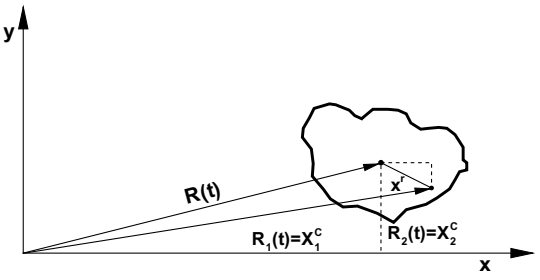

Fig. 6. Schematic presentation of relative and absolute frame of reference.

$$m_n^s(x, t) = \int\int\int_{\mathbb{R}^3} m_n^r(x^r, t) p_R(x - x^r; t)\, \mathrm{d}x_1^r\, \mathrm{d}x_2^r\, \mathrm{d}x_3^r \tag{19}$$

where $m_n^r(x^r, t)$ are relative frame of reference concentration standard moments evaluated by (12a)–(12c) using (13) with (14). In very early works on relative dispersion Gifford [20] assumed the Gaussian shape for the plume center position pdf. The similar conclusion was later followed by Kitanidis [24], Dagan [11], Pannone and Kitanidis [32], Zhang et al., [39] for subsurface concentration or in the solute flux approach by Andričević and Cvetkovic [3,4]. Recently, Ye and Wilson [38] also came to the same conclusion in the atmospheric turbulence problems. The assumed Gaussian shape for plume center pdf has spatial displacement variance evaluated, for example, with the second term on the right hand side of (14).

By solving (19), the comparison between concentration standard moments is depicted in Fig. 7, for two travel times ($\tau = 10$ and $\tau = 20$). The concentration standard moments evaluated on the plume center line, for the source $A_0(0.2, 1)$ and local dispersion strength of $a = 0.05$, demonstrate important concentration statistics behavior in the relative and absolute frame of reference. The relative framework concentration moments are 4–5 times higher in magnitude than moments in the absolute framework, for this example, indicating the degree of attenuation in the concentration moments magnitude created with large scale heterogeneity features (plume meandering). On the other hand the concentration moments in the absolute frame of reference have wider spatial support than relative framework moments indicating the important concentration uncertainty present in selecting the proper monitoring network design in space [2]. In addition, the bimodality feature observed in the relative framework concentration moments (especially for higher moments) is not any more present in the absolute framework moments, again, due to the plume meandering.

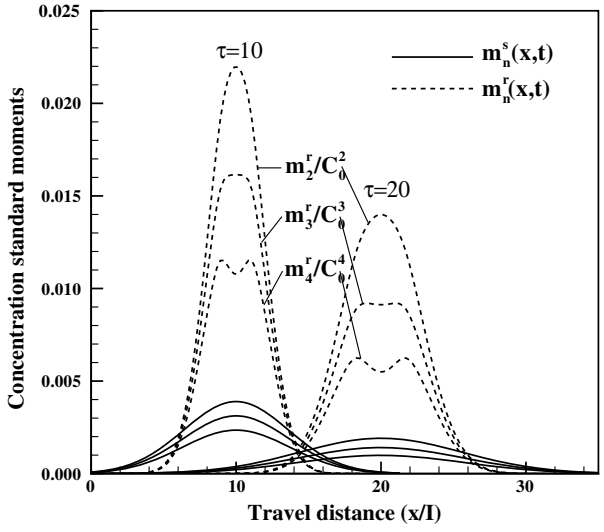

Fig. 7. Comparison of concentration standard moments in absolute and relative frame of reference for two mean travel times along the plume centerline.

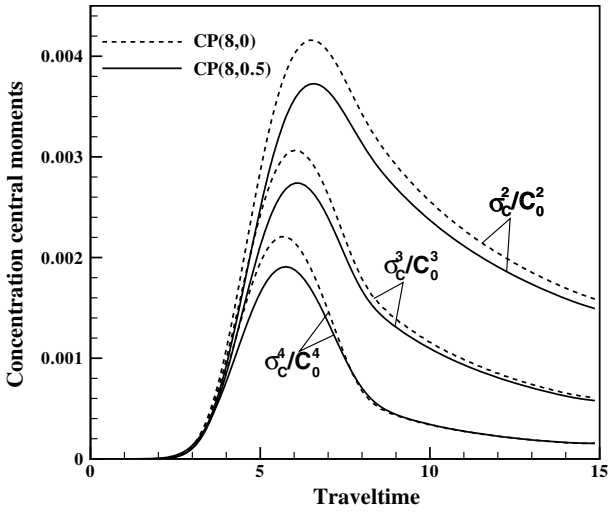

Fig. 8. Second, third and fourth concentration central moments in the absolute frame of reference as a plume passes two fixed control points CP(8, 0) and CP(8, 0.5).

In reality, of course, we have only one realization and relative framework moments clearly describe the internal plume fluctuation structure and actual concentration mass that could be experienced in the field by an observer. However, where this scenario will be taking place in the space is uncertain. This uncertainty results from the large scale heterogeneity and is quantified with plume meandering. Hence, both frameworks, absolute and relative, are providing crucial information needed in practice since the concentration fluctuations observed at a fixed point in space is combined result of internal mixing and plume meandering.

In Fig. 8 the concentration moments in absolute framework are present for two selected control points; CP(8, 0) and CP(8, 0.5). The magnitude of the moments presents the combined effect coming from the large and small scale velocity heterogeneity and can be seen as combined information consisting of uncertainty whether the plume will pass near the CP and what might be the internal plume fluctuation structure for that scenario. As expected, the CP(8, 0.5) placed one half $\ln K$ correlation scale off the x-direction has reduced concentration moments.

6. Concluding remarks

This paper proposed a simple, yet theoretically sound and consistent, method of evaluating any number of concentration moments in absolute and relative frame of reference for a plume subject to the heterogeneous velocity field in the subsurface. The derived second, third and fourth concentration central moments in (12a)–(12c) are functions of the mean concentration and pore scale dispersion responsible for the dilution process. The pore scale dispersion appears to have significant influence on the magnitude and shape of the concentration higher moments. The solution for the zero local dispersion case is a conservative envelope with concentration moments exhibiting unimodal shape whereas the solution with the non-zero local dispersion often becomes bimodal. This is particularly the case for larger local dispersion and higher concentration moments. The results from the numerical studies which are based on a detailed field experiment showed good agreement with proposed solution for the concentration variance.

Applying the spatial convolution principle a simple relationship between the relative and absolute framework concentration standard moments is presented. The comparison between concentration standard moments in the relative frame of reference and moments in the absolute framework revealed the practical importance of both. While relative framework moments are describing the internal fluctuation structure as seen by someone moving with the plume, the absolute moments are combining the plume meandering created from large scale heterogeneity and small scale heterogeneity responsible for internal plume structure. Both information are valuable in the practice. The internal fluctuation structure of the plume is critical in the proper assessment of the risk that might be affecting the population exposed to such plume structure. On the other hand, the plume meandering can not be just removed since for a fixed point observer the concentration fluctuations result from the internal mixing and plume meandering. Meandering of the plume is a relatively slow process compared to the internal plume mixing and may not play important role in the near field. Thus, the absolute framework moments are balancing out the unavoidable uncertainty coming from the plume meandering and plume structure development in one information which is particularly suitable for the monitoring network design and for establishing the environmental protection zones in the nature (e.g., wellhead protection zones).

The knowledge of first two concentration moments describes only the position and fluctuation size of the moving plume, while higher concentration moments are providing additional information for the extreme values that could be present in the tails of the concentration pdf. The ability to predict the concentration moments in practice for some accidental spills is valuable information, however, one often needs to know the point or block exposure concentration pdf for probabilistic risk assessment studies. The evaluation of such concentration pdf can be obtained using, e.g., maximum entropy formalism [15] or any other statistical techniques when at least four concentration moments are available. Besides estimating the concentration pdf, it is also important to determine the exposure duration of high concentration values or the injected mass at some point in space. Some of these aspects and evaluation possibilities in the practice deserve the future research efforts in order to improve the environmental risk assessment.

References

[1] Andričević R. Effects of local dispersion and sampling volume on the evolution of concentration fluctuations in aquifers. Water Resour Res 1998;34(5):1115–29.

[2] Andričević R. Evaluation of sampling in the subsurface. Water Resour Res 1996;32(4):863–74.
[3] Andričević R, Cvetković V. Evaluation of risk from contaminants migrating by groundwater. Water Resour Res 1996;32(3):611–21.
[4] Andričević R, Cvetković V. Relative dispersion for solute flux in aquifers. J Fluid Mech 1998;361:145–74.
[5] Barry DA. Supercomputers and their use in modeling subsurface solute transport. Rev Geophys 1991;28:277–97.
[6] Bellin A, Rubin Y, Rinaldo A. Eulerian–Lagrangian approach for modeling of flow and transport in heterogeneous geological formations. Water Resour Res 1994;30(11):2913–25.
[7] Burr DT, Sudicky EA, Naff RL. Nonreactive and reactive solute transport in three-dimensional porous media: mean displacement, plume spreading, and uncertainty. Water Resour Res 1994;30: 791–817.
[8] Caroni E, Fiorotto V. Analysis of concentration as sampled in natural aquifers. Transport Porous Media 2005;59:19–45.
[9] Chatwin PC, Sullivan PJ. A simple and unifying physical interpretation of scalar fluctuation measurements from many turbulent shear flows. J Fluid Mech 1990;212:533–66.
[10] Dagan G. Transport in heterogeneous porous formations: spatial moments, ergodicity, and effective dispersion. Water Resour Res 1990;26:1281–90.
[11] Dagan G. Dispersion of passive solute in nonergodic transport by steady velocity fields in heterogeneous formations. J Fluid Mech 1991;233:197–210.
[12] Dagan G. Flow and transport in porous formations. New York: Springer-Verlag; 1989.
[13] Dagan G, Fiori A. The influence of pore scale dispersion on concentration statistical moments in transport through heterogeneous aquifers. Water Resour Res 1977:1595–605.
[14] Dagan G, Fiori A, Berglund S, Cvetkovic V. A first-order analysis of solute flux statistics in aquifers: the combined effect of pore-scale dispersion, sampling, and linear sorption kinetics. Water Resour Res 2002;38(8):15. article 12.
[15] Derkson RW, Sullivan PJ. Moment approximation for probability density functions. Combust Flame 1990;81:378–91.
[16] Fiori A, Dagan G. Concentration fluctuations in transport by groundwater: comparison between theory and field experiments. Water Resour Res 1999;35(1):105–12.
[17] Fiori A, Dagan G. Concentration fluctuations in aquifer transport: a rigorous first-order solution and applications. J Contam Hydrol 2000;45(1):139–63.
[18] Fiorotto V, Caroni E. Solute concentration statistics in heterogeneous aquifers for finite Peclet values. Transport Porous Media 2002;48:331–51.
[19] Fitts CR. Uncertainty in deterministic groundwater transport models due to the assumption of the macrodispersive mixing: evidence from the Cape Cod (Massachusetts, USA) and Borden (Ontario, Canada) tracer tests. J Contam Hydrol 1996;23:69–84.
[20] Gifford F. Statistical properties of a fluctuating plume dispersion model. Adv Geophys 1959;6:117–37.
[21] Graham W, McLaughlin D. Stochastic analysis of nonstationary subsurface solute transport, 1. Unconditional moments. Water Resour Res 1989;25:215–32.
[22] Kapoor V, Gelhar L. Transport in three-dimensionally heterogeneous aquifers, 1. Dynamics of concentration fluctuations. Water Resour Res 1994;30(6):1775–88.
[23] Kapoor V, Kitanidis PK. Concentration fluctuations and dilution in aquifers. Water Resour Res 1998;34(5):1181–93.
[24] Kitanidis PK. The concept of dilution index. Water Resour Res 1994;30:2011–26.
[25] Kitanidis PK. Prediction by the method of moments of transport in a heterogeneous formation. J Hydrol 1988;102:453–73.
[26] Li S, McLaughlin D. A nonstationary spectral method for solving stochastic groundwater problems: unconditional analysis. Water Resour Res 1991;27(7):1589–605.
[27] Li S-G, McLaughlin D, Lio H. The accuracy of stochastic perturbation solutions to subsurface transport problems. Adv Water Resour 2004;27:47–56.
[28] Maxwell R, Pelmulder SD, Tompson FB, Kastenberg WE. On the development of a new methodology for groundwater driven health risk assessment. Water Resour Res 1998;34(4):833–47.
[29] Neuman SP. Eulerian–Lagrangian theory of transport in space–time nonstationary fields: exact nonlocal formalism by conditional moments and weak approximations. Water Resour Res 1993;29(3):633–45.
[30] Nielsen M, Chatwin PC, Jorgensen HE, Mole N, Munro RJ, Ott S. Concentration fluctuations in gas releases by industrial accidents. EU-DG environment. COFIN (ENV4-CT97-0629) project, 2002.
[31] Plata A. Parameters of carbonate rock aquifers from tracer methods. Hydrogeological Processes in karst terranes, IAHS Publ. No. 207, 1993.
[32] Pannone M, Kitanidis PK. Large-time behavior of concentration variance and dilution in heterogeneous formations. Water Resour Res 1999;38(3):623–34.
[33] Rajaram H, Gelhar LW. Plume scale-dependent dispersion in heterogeneous aquifers, 2. Eulerian analysis and three dimensional aquifers. Water Resour Res 1993;29(9):3261–76.
[34] Rubin Y, Cushey MA, Bellin A. Modeling of transport in groundwater for environmental risk assessment. Stoch Hydrol Hydraul 1994;8:57–77.
[35] Rubin Y. Applied stochastic hydrogeology. 1st ed. Oxford Press; 2003.
[36] Sawford BL, Sullivan PJ. A simple representation of a developing contaminant concentration field. J Fluid Mech 1995;289:141–57.
[37] Sullivan PJ. The influence of molecular diffusion on the distributed moments of a scalar PDF. Environmetrics 2004;15:173–91.
[38] Ye E, Wilson DJ. A comparison of the detailed structure in dispersing tracer plumes measured in grid-turbulence with a meandering plume model incorporating internal fluctuation. Bound-Layer Meteorol 2000;9:253–96.
[39] Zhang D, Neuman SP. Effect of local dispersion on solute transport in randomly heterogeneous media. Water Resour Res 1996;32:2715–25.